Role of clay minerals in the physicomechanical deterioration of sandstone

Inmaculada Jiménez-González,[1] Carlos Rodríguez-Navarro,[2] and George W. Scherer[3]

Received 29 June 2007; revised 31 January 2008; accepted 3 March 2008; published 7 June 2008.

[1] Extensive weathering suffered by sandstone in natural outcrops as well as in historical buildings could be attributed among other mechanisms to the action of wetting and drying cycles. We have recently shown how to quantify the stresses generated during such cycles to determine whether damage can take place. This procedure is further developed in this paper and applied to the *Tarifa sandstone*, a sandstone with a 7 wt % content of clay minerals and used in the main façade of the church of San Mateo in Tarifa (Cádiz, Spain) for which the relevant material properties are measured. It is shown that tensile stresses during drying can cause cracking of thin elements and that shear forces can cause buckling of wetted surfaces more generally, eventually resulting in scaling and/or contour scaling. These predictions are supported by visual observations on the monument showing degradation patterns characteristic of those types of damage. Similar weathering forms have been observed in natural sandstone landscapes. Application of swelling inhibitors (e.g., cationic surfactants) that selectively adsorb on the clay basal planes, results in a substantial swelling reduction. This confirms that the swelling clays typically present in sandstone are pivotal for its weathering and indicates that swelling inhibitors are a potentially valuable treatment to prevent or minimize damage to stone. The circumstances that would lead to weathering are discussed in relation to sandstone material properties in the wet and dry state. Clay-bearing stones are shown to exhibit softening during wetting, as well as viscoelastic stress relaxation, which is expected to limit the extent of damage. These results may aid in the better understanding of sandstone weathering both in nature and in urban environment and may help develop conservation methods to mitigate wetting/drying damage in ornamental sandstone or to prevent pore plugging in reservoir sandstones.

Citation: Jiménez-González, I., C. Rodríguez-Navarro, and G. W. Scherer (2008), Role of clay minerals in the physicomechanical deterioration of sandstone, *J. Geophys. Res.*, *113*, F02021, doi:10.1029/2007JF000845.

1. Introduction

[2] Sandstones represent a significant volume of Earth's surface rocks. *Meybeck* [1987] estimates that they cover ca. 15% of the emerged land surface, a value nearly similar to that of granite or limestones. Sandstones are also one of the most common ornamental stones used in the built and sculptural heritage [*Winkler*, 1997]. Weathering of sandstone is a critical geomorphological phenomenon that has shaped and currently shapes the landscape and surface features of, for instance, the Grand Canyon, Zion Canyon, Monument Valley, and Arches National Park in the United States [*Bradley*, 1963; *Robinson*, 1970; *Cruikshank and Aydin*, 1994], the carved city of Petra in Jordan [*Paradise*, 2002; *Heinrichs*, 2005], or a number of cathedrals across Europe [*Vicente*, 1983]. Sandstone weathering also results in the development of striking weathering forms such as pedestal rocks [*von Engeln*, 1942], honeycombs [*Mustoe*, 1982], tafoni or caverns [*Young*, 1987; *Sancho and Benito*, 1990], scaling and contour scaling [*Snethlage and Wendler*, 1997], and polygonal cracking [*Williams and Robinson*, 1989], whose origins are still a matter of debate [*Turkington and Paradise*, 2005]. However, while study of rock weathering and stone decay has mainly focused on granite or limestone decay, sandstone still remains a relatively overlooked landscape element and building stone [*Turkington and Paradise*, 2005].

[3] In recent years, geomorphological methods and studies on natural rock weathering have gained a prominent status in the conservation of stone cultural heritage [*Pope et al.*, 2002]. Conversely, research into rock weathering has been significantly advanced through the study of urban stone decay [*McGreevy and Whalley*, 1984]. There are several reasons for the study of stone decay as a useful analogy for rock weathering in natural settings. Among them, one is the availability of easily characterized stone in a dated monu-

[1]University of Granada, Granada, Spain.
[2]Department of Mineralogy and Petrology, University of Granada, Granada, Spain.
[3]Princeton Institute for the Science and Technology of Materials, Department of Civil and Environmental Engineering, Princeton University, Princeton, New Jersey, USA.

0148-0227/08/2007JF000845$09.00

ment, which enables an accurate study of weathering processes and rates [*Dragovich*, 1978; *Meierding*, 1981; *Pope et al.*, 2002; *Hoke and Turcotte*, 2002]. Another reason is the relative ease of performing laboratory and field tests using stone samples under well-established conditions that help single out a particular weathering mechanism [*Rodríguez-Navarro and Doehne*, 1999]. In the case of sandstone, case studies, laboratory tests, and field exposure trials have focused on the study of salt weathering [*Goudie and Viles*, 1997], frost shattering [*McGreevy*, 1981], black crust (gypsum) formation [*Smith et al.*, 1994], chemical weathering (including case hardening) [*Young*, 1987], thermal weathering [*Warke and Smith*, 1998] and biodeterioration [*Mottershead et al.*, 2003]. However, other weathering mechanisms such as expansion/contraction associated with wetting/drying phenomena [*Trenhaile*, 1987; *Yatsu*, 1988] have comparatively received less attention [*Hall and Hall*, 1996; *Delgado Rodrigues*, 2001].

[4] Sandstones typically contain clays in the cement that binds the grains together [*Tallman*, 1949; *Houseknecht and Pittman*, 1992]. This type of cementing phase makes them highly susceptible to deterioration, especially under conditions of cyclic wetting and drying that cause swelling and shrinkage of clay minerals. The literature on stone conservation provides numerous studies that point to this as a durability problem for sedimentary stones [*Beloyiannis et al.*, 1988; *Caner and Seeley*, 1978; *Delgado Rodrigues*, 2001; *Iñigo et al.*, 2003; *Kühnel et al.*, 1994; *Rodríguez-Navarro et al.*, 1997, 1998; *Pye and Mottershead*, 1995; *Wüst and McLane*, 2000; *Veniale et al.*, 2001; *Vicente*, 1983]. Studies on the durability of sandstones used for road pavement and other engineering purposes also suggest that clays may have a detrimental impact on their service life [*Dunn and Hudec*, 1966; *Fookes and Poole*, 1981]. Polygonal cracking [*Williams and Robinson*, 1989], tafoni [*Martini*, 1978], honeycombs [*Gill et al.*, 1980], and spalling/multiple scaling, as well as contour scaling [*Robinson and Williams*, 1994; *Heinrichs*, 2005] observed on sandstone outcrops in nature have also been related to the presence of clay minerals. However, the actual role of clays and wetting/drying events on the development of such weathering forms is a matter of controversy [*McGreevy and Smith*, 1984; *Turkington and Paradise*, 2005]. The lack of a physical-mechanical theory backed by experimental data, demonstrating the actual role of the swelling/shrinking of clay minerals in weathering of sandstone, may have fostered this controversy.

[5] Clay-containing sandstones used for building purposes can develop significant swelling strain. For instance, Spanish Cervelló and Villamayor sandstones that show severe damage in some historic buildings are reported to swell respectively by 5000 and 6700 μm/m [*Esbert et al.*, 1997] in the direction perpendicular to their bedding planes. In general, swelling strain values above 1500 μm/m can be considered quite large, since the product of this strain with the elastic modulus typically exceeds the tensile strength of the stone. However, as will be explained in this paper, swelling strain alone is not sufficient to determine whether swelling may cause damage. Factors that have to be considered include elastic modulus, viscoeastic relaxation rate, tensile, shear or compressive strength of the sandstone, and relative humidity. This approach could be successfully used to identify situations where a sandstone with rather limited dilatation would get damaged. For instance, severe damage occurs in Petra sandstone, which shows a maximum swelling strain of 700 μm/m [*Heinrichs*, 2005], and in Portland Brownstone, with 500 μm/m of swelling strain (this study). As detailed in section 4.3, the stresses in the latter case can be shown to exceed the strength of the stone. The role of clay distribution in the stone has also been pointed out to be important [*Dunn and Hudec*, 1966] since inhomogeneity could give much higher local strains and stresses.

[6] Although the problem has been often mentioned, quantification of the stresses arising from such wetting/drying cycles has only been discussed recently [*Jiménez-González and Scherer*, 2004; *Wangler et al.*, 2006]. Experimental evidence of the damaging character of these cycles was reported by *Rodríguez-Navarro et al.* [1997] and *Wendler et al.* [1996]. In the first case, the authors studied a clay-rich Egyptian limestone that basically decomposed when submerged in water. The study by *Rodríguez-Navarro et al.* [1998] is particularly important for museums in countries with climates more humid than Egypt. However, the properties of this stone remain very different from situations that can be encountered with building stones still in service in outdoor environments exposed to rain, or in natural outcrops. The case examined by *Wendler et al.* [1996] is closer to such situations. The authors examined the aging of stones from Easter Island by measuring the drill resistance of quarry samples subjected to wetting and drying cycles. They observed that these cycles very much reduced drill resistance in the outer layer of the samples. They also found that treating with diaminobutane dihydrochloride as a swelling inhibitor [*Wendler et al.*, 1991; *Snethlage and Wendler*, 1991] dramatically reduced the loss of drill resistance. This study highlights the fact that wetting and drying cycles can damage clay-bearing stones, but that swelling inhibitors can be used to mitigate this. Regarding the use of conventional conservation treatments, it has been reported that clay-bearing stones consolidated by ethyl silicates rapidly lose the consolidation effect after a limited number of cycles of wetting and drying, apparently as a result of hydric strain [*Félix and Furlan*, 1994; *Félix*, 1988, 1995].

[7] Over the past few years, we have examined the weathering of clay-bearing stones with the objective of analyzing the stresses generated during wetting and drying cycles in order to determine their potential for damaging action [*Jiménez-González and Scherer*, 2004; *Scherer and Jiménez-González*, 2005]. In this process we have introduced novel characterization techniques and improved others. These include warping of thin stone plates and accelerated swelling pressure measurements [*Jiménez-González et al.*, 2002; *Scherer and Jiménez-González*, 2005; *Jiménez-González and Scherer*, 2006]. We also applied the technique of beam bending under dry and saturated conditions to determine the viscoelastic character of these stones [*Jiménez-González and Scherer*, 2004].

[8] In this paper we apply all these methodologies to study a sandstone from the South of Spain that shows substantial damage on the façade of San Mateo Church in Tarifa (Cádiz, Spain). This type of stone is also to be found

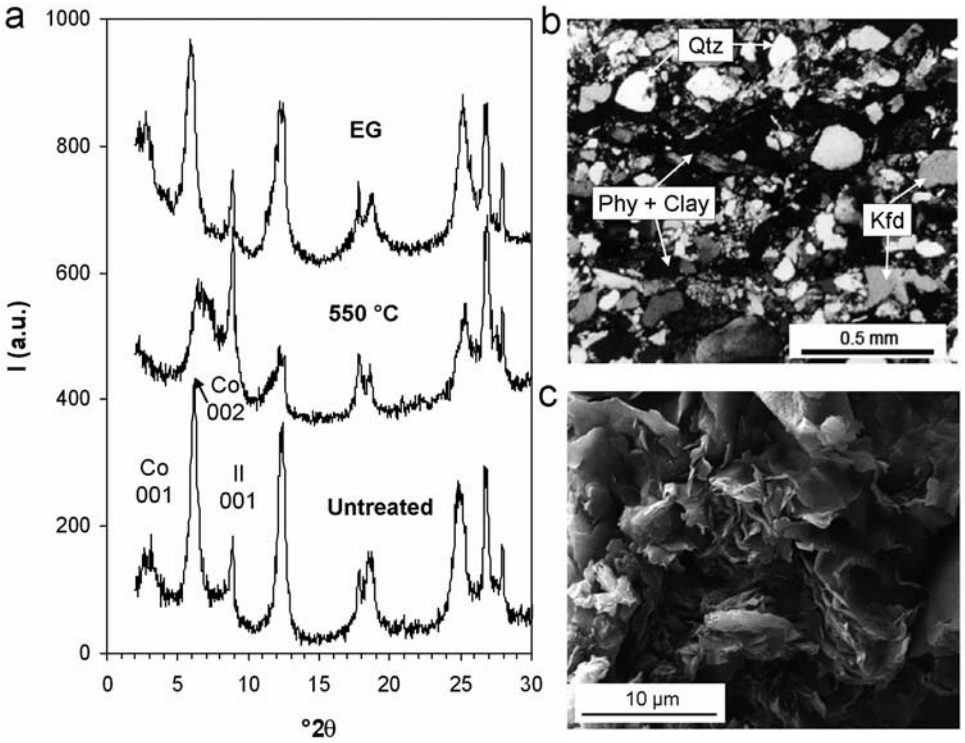

Figure 1. Mineralogy and texture of Tarifa sandstone. (a) XRD patterns of oriented aggregates showing illite (Il) 001 reflection and corrensite (Co) 001 and 002 reflections and their change upon glycolation (EG) and thermal treatment (550°C). (b) Representative optical microscopy photomicrograph (crossed polars) showing quartz (Qtz), potassium feldspar (Kfd), and phyllosilicates plus clays (Phy + Clay) oriented along bedding planes (horizontal). (c) SEM photomicrograph of the clay minerals.

on the nearby Roman ruins of ''Baelo Claudia,'' where it displays similar damage patterns [*Hoyos et al.*, 1999].

[9] Concerning the Church of San Mateo, *Sebastián et al.* [2008] describe the damage patterns as granular disintegration, flaking, scaling and ''contour scaling,'' as well as cracking of ornamental elements. They attribute this damage to the swelling and shrinking of clays and weaknesses of the stone resulting from its high anisotropy. Furthermore, they indicate that sodium chloride aerosols increase the hygroscopicity of the stone and favor the osmotic swelling of the clays.

[10] In the present study, our experiments demonstrate that we are using a valid theoretical analysis of how stresses develop in clay-bearing stones during cycles of wetting and drying. On the basis of these results, we determine under what conditions damage is likely to occur during such cycles on a monument or on a natural outcrop. We also examine the use of swelling reducing agents as a way to mitigate sandstone damage. Ultimately, we will show that the theoretical analysis and the study of the damage associated with wetting/drying of clay-bearing Tarifa sandstone could be extended to understanding sandstone weathering on Earth's surface as well as elsewhere (e.g., Mars).

2. Materials and Methods

2.1. Materials

[11] The stone object of this study is one of the most representative materials used in the main (south) façade of the San Mateo Church, in the town of Tarifa (Cádiz, Spain). It is an arkose sandstone whose matrix or cementing phase is composed prevalently of clays and a small proportion of carbonates. Generally, two varieties have been distinguished by *Sebastián et al.* [2008]: the light brown and the gray variety, the first one being the closest to the one used in this study.

[12] Samples were obtained from blocks extracted from the original quarries (currently closed) located near Tarifa. A description of these quarries is given by *Sebastián et al.* [2008]. Before all tests, the samples were oven dried (60°C) to constant weight and then stored in hermetic containers for cooling. For tests under saturated conditions, vacuum impregnation by water was additionally performed.

[13] Samples were studied by means of scanning electron microscopy (SEM; Zeiss DMS 950) and polarized light microscopy (PM; Jenapol V). Powder X-ray diffraction (XRD) analyses were performed on a Philips PW 1710 diffractometer equipped with a graphite monochromator and using Cu $K\alpha$ radiation (λ = 1.5418 Å). XRD analyses were performed on ground whole rock and oriented aggregates (untreated, ethylene glycol solvated and heated for 1 h at 550°C) of the clay fraction (size < 2 μm).

[14] This sandstone is composed mainly of quartz. Other minerals found in lesser amounts are feldspars, calcite and phyllosilicates, including muscovite, biotite and chlorite. Figure 1a shows XRD patterns of the clay fraction. Smectite-chlorite mixed layers (corrensite) and minor amounts of illite are the main clay minerals present, which shows average values of 7 wt %. The corrensite mixed layer clay

was identified by the increase in the d_{001} spacing from 28.3 Å up to 31.5 Å after glycolation and the collapse of the d_{002} spacing from 14.2 Å to a broad peak at 13 Å upon heating [*Wilson*, 1987].

[15] Clays can experience two types of swelling: intracrystalline swelling and interparticle or osmotic swelling [*Rodríguez-Navarro et al.*, 1998, and references therein]. The former is experienced by the so-called expandable or swelling clays, such as smectite or mixed layer smectite-chlorite and smectite-illite, which are very common in sandstones [*Houseknecht and Pittman*, 1992]. Intracrystalline swelling results in an increase of the d_{001} spacing when the clays are in contact with a polar liquid (e.g., water or ethylene glycol). Osmotic swelling is experienced by all clay minerals (expandable and nonexpandable clays) in the presence of an electrolyte [*Madsen and Müller-Vonmoos*, 1989]. Higher swelling strains are observed in rocks containing expandable clays than in rocks containing nonexpandable clays [*Yatsu*, 1988]. Regarding the swelling potential of corrensite, this clay was found responsible for the floor heave of tunnels in the Keuper formation of SW Germany [*Yatsu*, 1988, and references therein].

[16] Optical microscopy and SEM observations show that the phyllosilicates display a preferred planar orientation along the stone bedding planes (Figures 1b and 1c). The latter is responsible for the marked textural and structural anisotropy of this stone [*Sebastián et al.*, 2008]. The pore system of the sandstone is characterized by submicron pores (pore radii 0.5–0.02 μm) having an average total porosity of around 8–11% [*Sebastián et al.*, 2008].

[17] To demonstrate unambiguously that swelling strain in clay-containing sandstone is due to clay swelling, and at the same time, to reduce or mitigate the swelling experienced by the Tarifa sandstone, we used diaminoethane dihydrochloride ($C_2H_8N_2{\cdot}2HCl$). The use of such cationic surfactants was first discussed by *Snethlage and Wendler* [1991] and considered by *Wendler et al.* [1996] for the conservation of Eastern Island Moai sculptures. This product adsorbs at the negatively charged (001) planes of clays, establishing bonds between two adjacent particles, thus preventing/minimizing swelling [*Snethlage and Wendler*, 1991]. In our study we applied the product by partially immersing the samples in 5 wt % aqueous solution, drying to constant weight (60°C) and repeating the whole operation a second time. The treatment does not have major effects on other materials properties, such as sorptivity, elastic modulus or color.

2.2. Methods

[18] The potential for damage from swelling depends on the depth to which water penetrates, the magnitude of the swelling strain, and the stiffness of the wet and dry stone, so we need to characterize all of those properties. The depth of saturation during contact with water (e.g., in a flood or rain event) depends on the sorptivity, which is the rate of uptake per unit area; if water enters the rock by capillary rise, then the distribution of moisture within the body will depend on the competition between the rate of rise and the rate of evaporation. We measure the sorptivity by a direct method described in section 2.2.1 and an indirect method, warping analysis, described in section 2.2.3. Similarly, the strain resulting from the saturation of an initially dry stone is measured directly by a dilatometric method (section 2.2.1) and indirectly by warping (section 2.2.3). If the wet surface of a dry stone expands, it creates compressive stresses; conversely, if the dry surface of a saturated stone contracts, it causes tensile stress. To calculate the stresses, we must know the mechanical properties of the rock, which we investigate by several methods, described in section 2.2.2. A convenient way to determine the elastic modulus is to calculate it from the acoustic velocity in the rock, which is quickly and easily done in the field. Unfortunately, that method gives highly unreliable results for clay-bearing stone, as we demonstrate by comparing the results of acoustic measurements with static moduli obtained by three point bending measurements. Static measurements are more appropriate for predicting swelling stresses in stone, where the duration of the process (*viz.,* wetting and drying) is on the order of hours or days. Moreover, these measurements reveal that the stone is viscoelastic, particularly when wet, and this will have an important impact on the magnitude of the swelling stresses. One might reasonably argue that it is simpler to measure the swelling stress directly, rather than calculating it from the strain and viscoelastic modulus. Such direct methods were performed, as described in section 2.2.4, but the results are disappointing, because it is difficult to confine the sample so as to prevent a strain smaller than 0.1%. This problem is avoided by the warping method, where moisture is introduced through one face of a thin plate of stone: as the wet side expands, it is resisted by the dry side, which results in warping of the plate. An elastic (or viscoelastic) analysis of this simple geometry leads to an explicit prediction of the rate and magnitude of deflection. Fitting the theoretical expression to the data (deflection versus time) yields estimates of the swelling strain, sorptivity, and ratio of elastic moduli in the wet and dry stone. This measurement is fast and requires relatively simple equipment. Finally, to predict damage we must compare the stress to the strength of the rock, so we must measure the tensile strength of the stone when dry (section 2.2.2) and the compressive strength of the stone when wet (value provided by Dr. G. Cultrone (personal communication, 2007).

2.2.1. Hydric Properties

[19] The rate of water intake is measured by sorptivity tests in which a sample is fixed to the bottom of an electronic balance with a 0.001 g resolution connected to a computer for the data acquisition [*Scherer and Jiménez-González*, 2005]. A container with deionized water is then raised until the water touches the bottom of the sample. The mass change (Δm) per unit surface of the sample base (A) is plotted versus the square root of time and found to be linear. The height of rise, Δh, is related to the weight gain by $\Delta h = \Delta m/(A\phi\rho_L)$, where ϕ is the porosity and ρ_L is the liquid density; Δh increases in proportion to $\sqrt{t}$. From the slope and the apparent porosity determined from the mass change at the plateau, we determined the sorptivity (S) in units of $cm/s^{1/2}$ for comparison with the value obtained by applying equation (2) in the analysis of the warping experiments. Measurements were performed with the sample bedding placed normal to the water surface. Additional measurements were done with samples placed with the bedding parallel to the water surface.

[20] The linear expansion or free swelling strain (ε_s) of the stone is measured by using a homemade dilatometer

[*Jiménez-González and Scherer*, 2004]. Typical sample sizes were 35 × 10 × 10 mm. The expansion was measured in directions both parallel and perpendicular to the bedding, using the following procedure: (1) the sample is placed in a glass container, (2) a pushrod mounted on an LVDT (linear variable differential transformer) is lowered on top of the sample and at that point the data acquisition starts, and (3) deionized water is poured into the container until it reaches near the upper surface of the sample (but without covering it, so that air is not trapped inside). As soon as the sample gets wet, it starts swelling. The dilatation is measured by the LVDT until it is complete. The strain difference between the initial value and the plateau value is used to calculate the linear free swelling strain.

[21] Longitudinal expansion of the long thin plates used for warping measurements was obtained using the same instrument and procedure, but a special sample holder was designed to keep the samples vertical during the measurement without preventing their swelling [*Jiménez-González and Scherer*, 2006].

2.2.2. Mechanical Properties

[22] The tensile strength of the stone is obtained from indirect tensile strength tests (Brazilian tests). Cylindrical samples of 2 cm diameter and 5 cm length are placed horizontally between the two platens of an Instron® machine that compress the sample until failure [*Jiménez-González and Scherer*, 2004].

[23] This property was only measured on dry samples because tensile strength is most important during drying of decorative elements, as explained below.

[24] The dynamic elastic modulus is determined from ultrasound transmission velocity measured using a portable Pundit instrument operating at 54 KHz. Nitrile pads are used instead of vacuum grease as contact agents [*Jiménez-González and Scherer*, 2004]. Stones were measured both wet and dry. These measurements were performed on the received blocks before they were cut to make the smaller samples used in the other experiments. In each direction, three measurements were done and found to be very similar.

[25] Homemade three point beam benders are used for measuring static elastic modulus of oven dried and vacuum saturated samples. Typical sizes for samples were about 100 × 20 × 4 mm (dimensions are measured accurately for each sample). Each instrument is composed of a computer controlled in-line system that is placed inside an incubator [*Vichit-Vadakan*, 2002; *Jiménez-González and Scherer*, 2004]. The measurements are done by applying a given displacement cyclically and measuring the corresponding load. The samples used for this test were cut such that the bedding was normal to the sample length, so we obtain Young's modulus perpendicular to the bedding.

[26] Stress relaxation tests were performed with the same benders described above. In this case, a constant displacement is applied and the load is measured over time. This measurement gives information on the viscoelastic behavior of the stones [*Jiménez-González and Scherer*, 2004].

2.2.3. Warping

[27] A novel technique that we call "warping" or "the 3 in 1 test" was introduced in former studies as a quick measure of swelling strain, sorptivity and ratio of wet to dry modulus [*Scherer and Jiménez-González*, 2005; *Jiménez-González and Scherer*, 2006]. Briefly, it consists in measuring the upward deflection (warping) of a thin plate of a swelling stone, placed horizontally on two supports, that swells as a result of adding water on its upper surface. A piece of tape is placed around the perimeter of the plate to contain the water, and an LVDT is placed in contact with the center of the top surface of the plate. Water is quickly poured onto the upper surface and the deflection measured by the LVDT is continuously recorded by a computer. This LVDT is placed midway between the two sample supports to measure the maximum deflection during the warping process. The samples are about 100 × 20 × 4 mm (dimensions are measured accurately for each sample).

[28] This experiment can be analyzed following *Timoshenko*'s [1925] approach where the sample is considered as an assemblage of two layers (1) the wet upper layer that tries to reach the maximum swelling (free swelling strain) and (2) the dry lower layer that tries not to expand.

[29] The combination of one layer trying to expand and the other resisting leads to warping with a deflection, Δ(cm), that depends on the relative depth of water penetration, d, on the free swelling strain, ε_S, and on the ratio of wet to dry modulus, r,

$$\Delta = \left(\frac{3w^2\varepsilon_S}{4h}\right) \cdot \left(\frac{r(1-d)d}{d^4(1-r)^2 - 4d^3(1-r) + 6d^2(1-r) - 4d(1-r) + 1}\right), \tag{1}$$

where w (cm) is the span and d can be written as a function of sorptivity, S (cm/s$^{1/2}$), plate thickness, h (cm), and time, t (s),

$$d = \frac{h_w}{h} = \frac{S}{h}\sqrt{t}, \tag{2}$$

where h_w (cm) is the wet part of the sample thickness.

[30] It is important to note that we do not have an independent measure of d. Its variation with time could therefore be different from what is given in the above equation, in particular for thin samples. Such a situation was found with another stone (the *Portland Brownstone*) and a model was proposed to analyze this [*Jiménez-González and Scherer*, 2006]. However, as explained later in the paper, equation (2) can be considered suitable for analyzing *Tarifa sandstone* samples.

[31] The free swelling is found directly from the maximum deflection, Δ_{max} and can be calculated by

$$\varepsilon_S = \frac{16}{3}\frac{\Delta_{max}h}{w^2}. \tag{3}$$

[32] The effects of sorptivity and the modulus ratio cannot be easily separated one from the other, which is why we choose to fit the curve simultaneously for both these parameters, after having determined the free swelling strain from the maximum deflection. Samples used for warping were cut so that some had the bedding perpendicular and others had it parallel to the surface onto which the water was poured.

2.2.4. Swelling Pressure

[33] Direct measurements of swelling pressure are performed by applying an external load to prevent the sample from swelling [*Madsen and Müller-Vonmoos*, 1985]. We

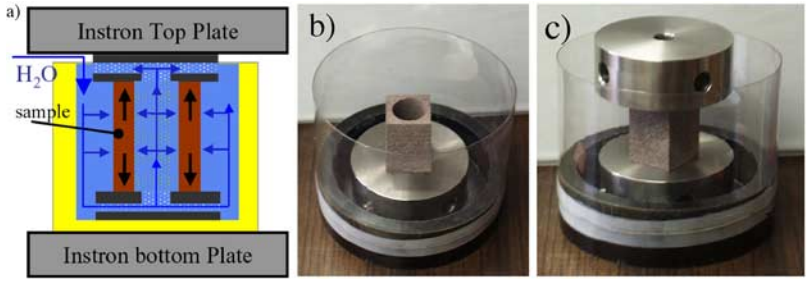

Figure 2. Illustration of the direct measure of swelling pressure setup. (a) Sketch showing how water infiltrates the sample core. (b) Image of the cored sample resting on the stainless-steel-perforated base. (c) Image of the sample as placed in the Instron machine. These pictures were taken with a sample having a square outer section unlike the one used in this study that has a circular one.

introduce changes in the sample size and geometry that greatly speed up the test (that now takes a couple hours instead of approximately two weeks). For that, we first used hollow parallelepiped samples with a square external section (as shown in Figure 2b). Afterward, as for this paper, we turned to hollow cylinders of similar dimensions (4 cm of outer diameter, 2 cm of inner diameter and 5 cm height), which facilitate the analysis of the experiment. The sample is placed between two stainless steel pieces that are drilled so as to let the water invade the sample from the inside (Figure 2a). The whole set up is placed in a container that has a stainless steel base (Figure 2c) and is positioned between two metal platens of the Instron machine described before. Initially both platens exert just enough pressure to keep the sample in place when water is added. The machine is instructed to maintain this initial position throughout the test. After adding water, the stone expands, so the load required to maintain a constant height increases and is stored on the computer. In this case, the bedding planes are horizontal, so that the swelling that is restrained is the one normal to the bedding (the maximum one) and water ingress is controlled by the sorptivity in the direction parallel to the bedding.

3. Results

3.1. Hydric Properties

[34] Our tests show that the capacity of the stone to absorb water by capillarity is relatively moderate with average rates of water ingress of 0.013 cm/s$^{1/2}$, and a sorption plateau at about 12% by volume (measured with the sample bedding normal to the water surface). It has been observed that sorptivity values change with the direction of water ingress (normal or parallel to the bedding planes). For the "brownish variety" measured values of rate of water ingress range from 0.008 cm/s$^{1/2}$ up to 0.015 cm/s$^{1/2}$ in directions perpendicular and parallel to the bedding, respectively.

[35] The free swelling strain in the direction parallel to the bedding averages 1.2×10^{-3} (or, 1200 μm/m) (Figure 3). It is substantially higher, about 2900 μm/m, in the direction perpendicular to the stone stratification (Figure 3). The 90% confidence limits, shown in Figure 3, are about ±200 μm/m. This value is slightly lower than the 3200 μm/m we previously reported [*Jiménez-González and Scherer*, 2004]. The difference is, however, much larger with the 4000 μm/m reported by *Sebastián et al.* [2008] for the *brown sandstone* variety. This large discrepancy is probably due to natural variations in the structure and composition of the blocks from which the samples were obtained. Indeed, we find that swelling measurements are quite reproducible on a given sample, but that sample-to-sample variations are much larger. These are also larger in the direction parallel to bedding (standard deviation 26% of the average) than in the direction of maximum swelling (standard deviation 10% of the average). This can be seen in Figure 3, where the 90% confidence intervals on swelling strain averages in both directions are also shown.

[36] The sample-to-sample variations can be problematic for the validation of the warping technique where an independent measurement of swelling strain is needed. For this reason, we directly measured the swelling strain (in the direction normal to the bedding planes) on the thin plates used for warping tests. We find values of around 2600–2800 μm/m, which are slightly lower than the overall average of 2900 μm/m reported above.

[37] On samples of Portland brownstone treated with the selected swelling inhibitor, the swelling strain (measured in the direction normal to the sample bedding) was reduced by 50% [*Jiménez-González and Scherer*, 2004].

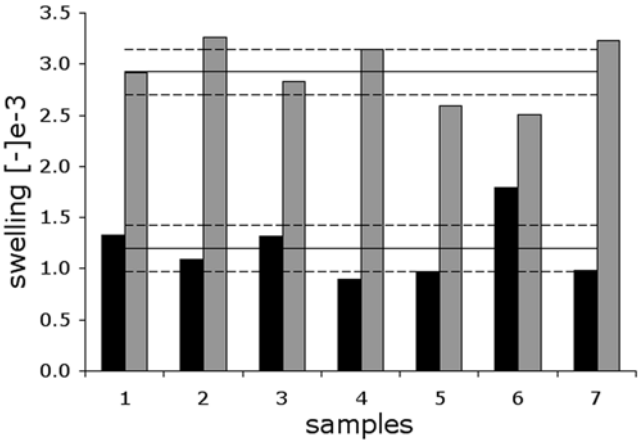

Figure 3. Free swelling strain measurements. Black and gray bars are averages of samples measured parallel and perpendicular to the bedding, respectively. The solid lines are the averages in both directions. The dashed lines show the associated 90% confidence interval on these averages.

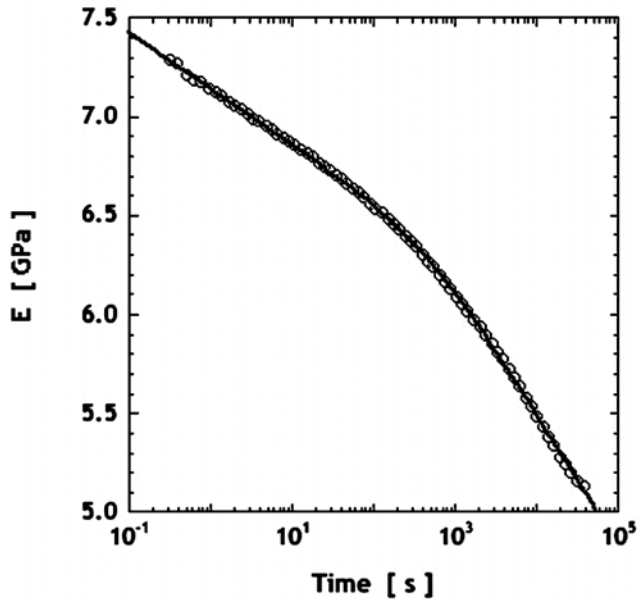

Figure 4. Stress relaxation of dry and untreated Tarifa sandstone (the sample bedding is parallel to the displacement applied). Circles indicate data points, and the solid curve indicates the fit by using equation (4).

3.2. Mechanical Properties

[38] In the direction perpendicular to the bedding, the average tensile strength is 5.3 MPa. In the parallel direction, an average value of 6.9 MPa was obtained.

[39] We have shown [*Jiménez-González and Scherer*, 2004] the existing discrepancy between dynamic and static elastic modulus on clay-containing stones. In the case of the *Tarifa sandstone*, this difference is very big: dynamic moduli are about 2 times greater than the static moduli for the dry stones (average of at least 5 samples, giving a standard deviation of about 15%). In the direction perpendicular to the bedding the dry static modulus is on average about 9.4 GPa while the dynamic modulus is 15.4 GPa. For water saturated samples the difference is much bigger, around 20 times. The average static modulus of the saturated stone is 0.9 GPa (average of two samples, standard deviation of about 15%) compared to the 19.6 GPa obtained from ultrasound velocity measurements.

[40] Samples treated with swelling inhibitor show no change of static dry modulus with respect to the untreated. For the saturated samples, the treatment seems to raise the static modulus by about 0.17 GPa, (around 20%) which is not negligible, given the very low wet modulus of this stone.

[41] In the direction parallel to the bedding, only the dynamic elastic modulus was measured. The dry and wet moduli are 28.4 and 27.5 GPa, respectively. However, these values should not be used to calculate stresses, because they drastically overestimate the elastic modulus.

[42] Stress relaxation measurements on dry samples (treated or untreated) show a bilinear relaxation rate on a logarithmic scale as represented in Figure 4.

[43] The stone relaxation involves two consecutive regimes, which can be fitted by using the following function:

$$E_d(t) = E_d(0) - a\ln\left(1+\frac{t}{\tau_1}\right) - b\ln\left(1+\frac{t}{\tau_2}\right), \qquad (4)$$

where $E_d(t)$ is the dry modulus at time t, $E_d(0)$ is the extrapolated dry modulus at $t = 0$, τ_1 and τ_2 are the characteristic times of the relaxation regimes of the dry stone and a and b are associated fitting constants.

[44] Early stress relaxation is governed by a and the later relaxation by b (Table 1). This implies that parameter a is the one that really characterizes the rate of stress relaxation in laboratory experiments (short test duration). The error for a is rather small (standard deviation of 15%, 2 samples treated, 4 samples untreated). Errors for the characteristic times, as well as for b, are larger (standard deviation between 38 and 75% of the average).

[45] In the case of water-saturated samples (Figure 5) subjected to bending, two relaxation processes occur: viscoelastic relaxation of stress in the solid and hydrodynamic relaxation of pressure in the pore fluid. The first process is similar in nature to that suffered by the dry samples, but with different kinetics. The extent of this relaxation continuously increases with time; on the other hand, the extent of the hydrodynamic relaxation is limited to a maximum value. When the sample is bent, the upper part of the sample is compressed (the water is squeezed out of that part) while the bottom is stretched (water is sucked into that part). This creates a pressure gradient and as a consequence the liquid in the sample redistributes. As this happens, the pressure gradient decreases, which means that the load needed to keep the sample bent decreases to a fixed value (for elastic materials). The rate at which the load decreases can be used to determine the sample permeability [*Scherer*, 2000, 2004; *Vichit-Vadakan and Scherer*, 2000, 2002].

[46] The stress relaxation measurement for wet samples is well fitted by a product of two functions, one describes the hydrodynamic relaxation and is denoted by $R(t)$, and

Table 1. Stress Relaxation Parameters for Dry and Saturated Tarifa Sandstone, Treated or Untreated

	Untreated							Treated						
	E_0 (GPa)	a (GPa)	b (GPa)	β (dimensionless)	τ_{VE} (s)	τ_1 (s)	τ_2 (s)	E_0 (GPa)	a (GPa)	b (GPa)	β (dimensionless)	τ_{VE} (s)	τ_1 (s)	τ_2 (s)
Dry	8.3	0.16	0.45	–	–	0.25	700	8.4	0.17	0.14	–	–	5.30E−4[a]	315
Wet	0.83	–	–	0.16	9.20E+7	–	–	0.84	–	–	0.57	1.30E+4	–	–

[a]Read 5.30E−4 as 5.30×10^{-4}.

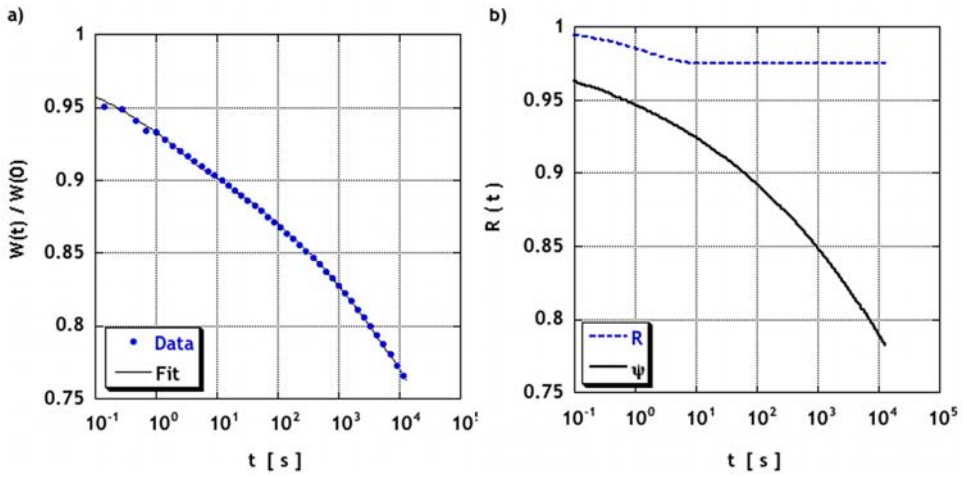

Figure 5. Stress relaxation of untreated water-saturated *Tarifa sandstone* that shows (a) the experimental data already fitted with equation (5) and (b) the deconvolution of the fitting function into the hydrodynamic (dashed curve) and the viscoelastic part (solid curve).

another that describes the viscoelastic relaxation and is denoted by $\psi(t)$

$$\frac{E_w(t)}{E_w(0)} = \frac{W(t)}{W(0)} = R(t)\psi(t), \tag{5}$$

where $W(t)$ and $E_w(t)$ are respectively the load and wet elastic modulus at time t, and $W(0)$ and $E_w(0)$ are respectively the load and wet elastic modulus at time $t = 0$. The type of function that is found to best fit the relaxation of wet samples is a stretched exponential

$$\psi(t) = \exp\left(-\left(\frac{t}{\tau_{\mathrm{VE}}}\right)^{\beta}\right), \tag{6}$$

where τ_{VE} is the characteristic time for the viscoelastic relaxation of the wet sample and β is a fitting parameter of the viscoelastic relaxation function.

[47] Results of stress relaxation tests performed on saturated and untreated Tarifa samples are shown in Figure 5. In Figure 5a, the experimental curve is shown to be well fitted with equation (5). In Figure 5b, the theory is used to deconvolve the data to show separately the hydrodynamic, $R(t)$ and viscoelastic relaxation, $\psi(t)$. A repetition of this test with the same sample gave errors of the fitting parameters between 1 and 7%. Larger values are obtained for sample to sample variation. For this reason the same sample was treated and measured again to see the effect of treatment.

[48] Relaxation rate averages for the saturated sample before and after treatment are given in Table 1 along with the corresponding moduli. In the saturated case, which we discuss later, the treatment with swelling reducing agents leads to a spectacular increase in the rate of relaxation as can be seen in Figure 6. We expect that this is due to a lubrication of the contacts between clay particles and/or layers by the swelling inhibitors. As discussed later, this should limit the maximum stresses reached during wetting and reduce damage. However, the effect of this treatment on the strength of the wet stone (in particular at slow loading rates) should also be evaluated. As an example of the importance of this issue, *Dunning et al.* [1980] and *Dunning and Huf* [1983] report significant time of failure reductions under compressive stress for sandstones impregnated with DTAB, which they attribute to interfacial energy reduction.

3.3. Warping

[49] From the warping curves (Figure 7), we extract values of swelling strain, ratio of wet to dry modulus and sorptivity. The maximum deflection can be used to calculate the free swelling strain from equation (3), which yields values of 2000 to 2500 μm/m. Direct measurements of free swelling strain on two samples used for warping gave similar results, lower than the overall average of 2900 μm/m obtained with smaller samples. For these two samples, the

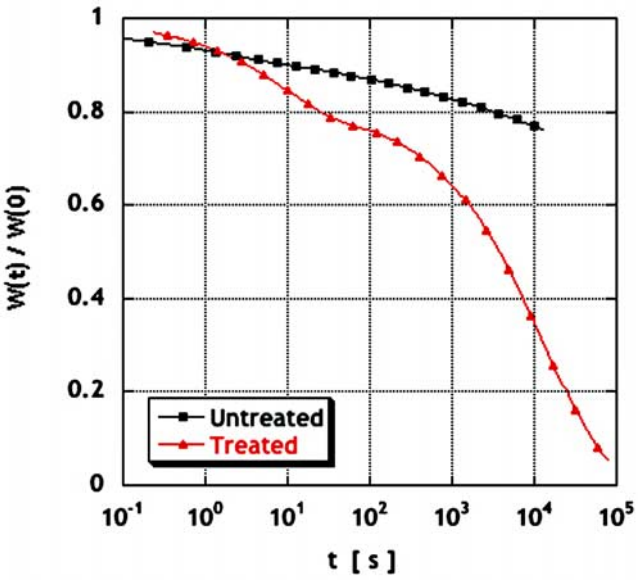

Figure 6. Fitted stress relaxation curves of untreated (squares) and treated (triangles) water-saturated *Tarifa sandstone*. Both curves are obtained from the same sample before and after treatment.

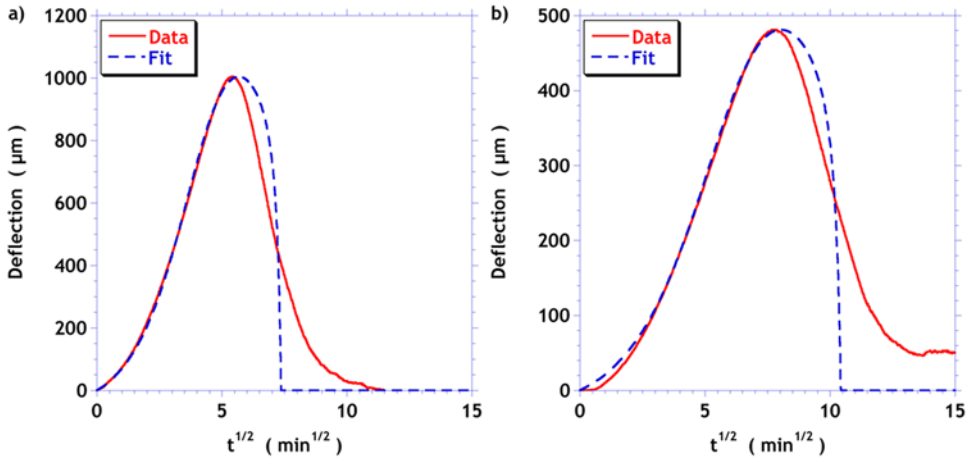

Figure 7. Warping curves of two *Tarifa sandstone* samples. (a) Bedding parallel to the water ingress. (b) Bedding perpendicular to the water ingress. The solid curve indicates the data points, and the dashed curve indicates the fit.

differences with the values obtained from warping were between 3 and 20%.

[50] With those values of maximum swelling, the first part of the warping curve is then very well fitted with equations (1) and (2) by adjusting sorptivity and modulus ratio. However, this is not the case for the second part, as already found for other stones [*Jiménez-González and Scherer*, 2006]. That discrepancy is a consequence of the kinetics of swelling and softening of the stone, together with effects of capillary pressure in the pores (P. Duffus et al., Swelling damage mechanism for clay-bearing sandstones, paper to be presented at the 11th International Congress on Deterioration and Conservation of Stone, Torun, Poland, 15–20 September, 2008, hereinafter referred to as Duffus et al., paper to be presented, 2008).

[51] For the three samples measured, the average fitted values of the swelling strain, ratio of wet to dry modulus (E_w/E_d), and sorptivity in directions parallel, and perpendicular to the bedding are given in Table 2.

3.4. Swelling Pressure

[52] The result of the direct swelling pressure measurement is shown in Figure 8. The final pressure is about 0.84 MPa. In that plot, the two vertical dashed lines are estimations of the time to saturation. The first one is the intersection between the horizontal line of the plateau and the dashed line of the maximum slope. The second one is a visual estimate of when the plateau pressure is reached. These estimates of saturation time, t_{sat} can be used to calculate sorptivity from the following equation [*Scherer and Jiménez-González*, 2005]:

$$t_{sat} \cong \frac{1}{4}\left(\frac{r_o - r_i}{S}\right)^2, \tag{7}$$

where r_i and r_o are the inside and outside radius of the sample respectively.

[53] Equation (7) and the saturation times estimated from Figure 8 give sorptivities of 0.0065 and 0.0082 cm/s$^{1/2}$. These values are very similar to the ones obtained from warping measurements, but smaller than the ones obtained from direct sorptivity measurements (0.013 cm/s$^{1/2}$). The possible cause of this difference is discussed in section 4.1.

4. Discussion

[54] In the first part of this section, we examine the warping and swelling pressure measurements using a mechanical analysis of differential stresses and strains in a swelling sample. This analysis accounts for these measurements very well, so we have confidence in the general validity of this treatment of a swelling stone.

[55] In the second part of this discussion section, we use that same analysis to evaluate under what conditions the *Tarifa sandstone* can be damaged by wetting and drying cycles. We also discuss the quantitative benefit of swelling inhibitor treatments for reducing damage.

[56] Finally, we discuss the implications of this study for better understanding of physical weathering due to wetting/drying of sandstones in both urban environments and on the Earth's surface (and beyond).

4.1. Warping

[57] As already shown by *Jiménez-González and Scherer* [2006], we cannot provide yet a total good fitting for the whole plot, but only for the first part of the curve which corresponds to the time at which the sample reaches the maximum deflection. The further sample relaxation could be probably explained by delayed expansion of the clays,

Table 2. Average Values of Swelling Strain, Ratio of Wet to Dry Static Modulus (E_{wet}/E_{dry}), and Sorptivity Obtained From the Fit of the Warping Curves

	Swelling Strain (μm/m)	E_{wet}/E_{dry} (dimensionless)	Sorptivity (cm/s$^{1/2}$)
Bedding parallel to the water ingress	2254	0.088	0.0072
Bedding perpendicular to the water ingress	1000	0.081	0.0039

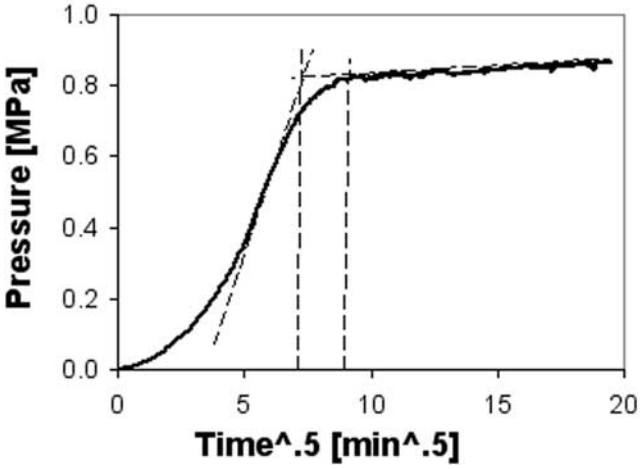

Figure 8. Swelling pressure evolution versus square root of time for a hollowed Tarifa cylindrical sample with 10.8 and 19.9 mm inner and outer radii, respectively.

together with the effect of capillary pressure, but we do not have yet a good way of accounting for this.

[58] From the maximum deflection, we calculate the maximum free swelling strain of the stone by using equation (3). That value, as already mentioned, agrees within 3–20% with the ones obtained by directly measuring that property on the same samples used to perform warping tests. Such a good agreement has not been reached with other stones (e.g., *Portland Brownstone*), although it is expected that the agreement should improve with thicker and longer samples.

[59] With the free swelling strain estimated from the maximum deflection, we then fit the first part of the warping curve by using equations (1) and (2) and adjusting the values of wet to dry modulus ratio and sorptivity.

[60] We find relatively good agreement between the ratio of wet to dry modulus extracted from warping measurements (0.088) and the one measured directly (0.095). The latter value is an average of beam bending measurements performed on different samples than the ones used for warping.

[61] Last, the sorptivity value that is extracted from warping (about 0.0072 cm/s$^{1/2}$) is consistent with the range estimated from swelling pressure tests (0.0065 to 0.0082 cm/s$^{1/2}$). However, these values differ substantially from the separate sorptivity measurements (around 0.013 cm/s$^{1/2}$). This discrepancy could be due to delayed swelling. Indeed, the analyses of both the swelling pressure and warping experiments assume instantaneous swelling, so that the progress of swelling can be determined directly by sorptivity. If the swelling were delayed, then the sorptivity calculated from these experiments would be lower, which is indeed the case. Sample to sample variation is not thought to explain this sorptivity difference, since independent measurements by *Sebastián et al.* [2008] were very similar to ours (0.016–0.018 cm/s$^{1/2}$).

[62] The largely nonlinear shape of the warping curve versus square root of time and the shift of the maximum deflection to longer times are due to the severe softening of the stone. It shows that the maximum swelling is only reached when a large part of the sample has been saturated. In terms of monument durability, it implies that large pressures only develop during wetting when a very large part of the block gets wet. These aspects are further discussed below.

4.2. Swelling Pressure and Stress Relaxation

[63] As mentioned in the previous section, sorptivity values extracted from swelling pressure measurements are consistent with the ones obtained from warping but not with the ones directly measured. Apart from this, the analysis of this experiment suggests that the pressure should increase linearly with the square root of time, which is not the case in Figure 8. This might be due to the top surface of the sample not being flat. If that is the case and because of the stone softening, the sample surface would first be pushed into (better) contact with the platens before being able to exert pressure.

[64] This possible issue of contact (smaller contact surface than sample surface) could also explain in part why the maximum pressure is only 0.83 MPa, which does not agree with the stress expected from the product of the wet modulus and free swelling strain (2.62 MPa). Even if stress relaxation is taken into account [*Scherer and Jiménez-González*, 2005], the calculated pressure is still substantially higher (2.18 MPa).

[65] Sample to sample variation in material properties does not seem a sufficient reason to explain this difference since the 90% confidence interval on this pressure is about 0.7 MPa.

[66] However, we observe that part of the curve is linear with square root of time as expected from the theory. This might correspond to the moment where the platens have a good contact with the sample. Extrapolation of this portion of the curve gives a pressure increase of 1.43 MPa between time zero and saturation. This corresponds to an intercept of −0.6 MPa that is just interpreted as a problem of setting the proper zero in a sample that does not have a perfect contact with the platens. This represents an attempt to obtain a more reliable estimate of the true swelling pressure (if the contact between the sample and the platens were perfect). This is much closer to the pressure calculated using viscoelastic relaxation and almost in range with the 90% confidence interval. However, the discrepancy remains large, which reflects the difficulty in achieving perfect experimental conditions for this type of measurement.

4.3. Stress Evaluation

[67] In this section we calculate the stresses that can develop during cycles of wetting and drying on clay-bearing stones. The hypotheses behind the equations presented are similar to those that led to the equation for analyzing the warping and swelling pressure experiments, which have been largely validated in the previous sections.

4.3.1. Compressive and Shear Stresses

[68] The maximum compressive stresses during wetting, σ_w, in the outer layer of an otherwise dry stone block can be estimated by (see Appendix A)

$$\sigma_w = \frac{E_w \varepsilon_S}{1 - \nu_w}. \tag{8}$$

Assuming a Poisson's ratio for the wet stone, ν_w of 0.2, and using the previously determined values of free swelling

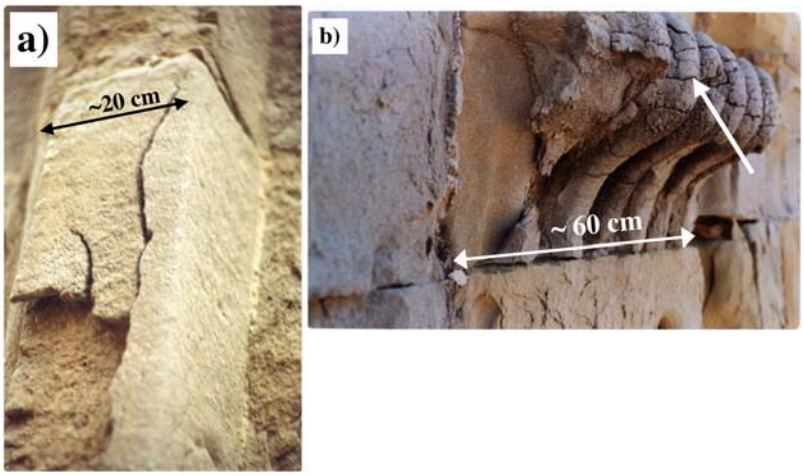

Figure 9. Possible damage patterns due to wetting and drying cycles on Tarifa sandstone. (a) Buckling of the stone surface during wetting. (b) Cracking of the stone surface following a mud-cracking pattern. The dimensions indicated are approximate.

strain, ε_S and elastic modulus of the wet stone, E_w, the calculated stress is 3.3 MPa in the direction perpendicular to the bedding.

[69] As explained before, damage during wetting could happen if those stresses overcome the wet compressive strength of the stone. This is not the case since the compressive strength normal to bedding planes was measured to be about 14 MPa in the wet state, (information provided by Dr. G. Cultrone (unpublished data, 2007)). It is important, however, to emphasize that this compressive strength could be substantially lower if determined with very slow loading rate because of the viscoelastic behavior of the stone. In view of Figure 6, which shows a strong acceleration of stress relaxation of treated samples, it appears that the role of loading rate on wet compressive strength on such samples is a subject to examine carefully in future studies.

[70] On the other hand, shear forces that develop during wetting could be responsible for cracks opening parallel to the stone surface. This can create a disruption between the dry and wet layers producing the buckling of the wet outer surface [*Scherer*, 2006] and resulting in scaling, or contour scaling. This is indeed observed in Figure 9, which is a strong indication that clay swelling is contributing to the degradation of the stone. For this mechanism of damage the quantification is unfortunately not very easy. What can be said is that buckling damage is facilitated by the presence of preexisting flaws (Duffus et al., paper to be presented, 2008). These can be inherent to the stone (e.g., bedding planes of face-bedded blocks). Indeed *Sebastián et al.* [2008] report not only that the church of Tarifa shows the detachment of plates several centimeters wide but also that this is particularly pronounced in face-bedded blocks. Alternatively these flaws maybe produced by other degradation mechanisms. Given the climate of Tarifa, freezing is not an issue. Furthermore, *Sebastián et al.* [2008] concluded that salt crystallization was not relevant, since the façade was only found to contain minor amounts of sodium chloride. However, considering that salt crystallization would only have to initiate damage, the role of this mechanism maybe much more important than one can conclude when considering it as a unique cause of damage.

4.3.2. Tensile Stresses

[71] During drying cycles, maximum tensile stresses, σ_d, in the outer layer of an otherwise wet stone can be estimated in a similar way as with equation (8) (see Appendix A)

$$\sigma_d = \frac{E_d \varepsilon_S}{1 - \nu_d}. \tag{9}$$

[72] Assuming a Poisson's ratio for the dry stone, ν_d of 0.2 (as for the wet stone) and using the previously determined swelling strain and dry modulus, we find stresses of about 34 MPa in the direction perpendicular to the bedding. This value exceeds by far the tensile strength of the stone (5.3 MPa) measured in the same direction. The same is true in the direction parallel to the bedding planes. However, in this case, we have to estimate the dry static modulus since no measurements are available. Using the same modulus as perpendicular to the bedding, stresses of 14 MPa are obtained, which exceed the tensile strength in that direction (6.9 MPa). These stresses rise to 26 MPa if we assume that the ratios of static and dynamic modulus are the same in both directions.

[73] These calculations seem to indicate that damage should always happen during drying. However, for tensile stress to develop, the stone must first be sufficiently expanded, which will only occur if a block or ornamental piece is almost completely saturated. For a block of thickness L we can calculate the depth of wetting L_w that must be achieved for drying stresses to reach the tensile strength of the stone in a thin external layer by using equation (10) (see Appendix A)

$$\sigma_{d,2} = \frac{E_d \varepsilon_S}{1 - \nu_d} \left(\frac{r}{r + \dfrac{L - L_w}{L_w}} \right), \tag{10}$$

where $\sigma_{d,2}$ is the tensile stress in the drying outer layer; ν_d is the Poisson ratio of the dry stone, $r = E_w/E_d$; E_d and E_w are the dry and wet static modulus, respectively, and ε_s is the free swelling strain of the stone.

[74] In the case where swelling takes place perpendicular to the bedding and for a 25 cm thick block, we find that the depth of wetting would have to be about 16 cm for drying

stresses to reach the stone tensile strength in that direction. This is an improbably large extent of wetting, since *Sebastián et al.* [2008] estimated that capillary rise of the waterfront is not very high in *Tarifa sandstone* and that water only penetrates superficially to a depth estimated to be about 2 cm. This mode of failure therefore only seems probable for thin ornamental elements that can get fully saturated. Such situations are illustrated in Figure 9b, where the cracks are of mud-cracking type, as would be expected if drying stresses are indeed causing damage. It is also important to note that *Sebastián et al.* [2008] described exactly this type of damage on ornamental features of the Tarifa Church façade.

[75] Other factors that can reduce the calculated stresses are slow drying (which permits viscoelastic relaxation) and a humid environment (which inhibits drying). However, the Town of Tarifa is known to be one of the windiest places in Europe, so that slow drying is no issue. In addition, the climate of the city is rather dry for a coastal location (average 75% RH according to *Hoyos et al.* [1999]). Overall, the main factor limiting drying stresses really appears to be the depth of wetting.

[76] Our calculations are based on the assumption of the stone having homogeneous properties. In fact, we believe that the scatter of data shown in Figure 3 reflects true heterogeneity of the stone. In consequence, it must be pointed out that very high local stresses could develop from differential strains on a millimeter scale.

4.3.3. Swelling Inhibitors

[77] The major effect of swelling inhibitors is to reduce the swelling strain. Consequently, with a 50% reduction in dilation, we expect a 50% reduction in stresses (tensile, compressive or shear). In the case of swelling pressure, the change in modulus of the wet treated stone, although small, is not negligible. Therefore the reduction of ε_s in equation (9) is partially offset by the increase in E, so the effective reduction in swelling pressure would be only 33%. On the other hand, the increase in viscoelastic relaxation would partially compensate this: in the swelling pressure measurements, it would contribute to an overall pressure reduction of about 44%. For similar reasons, the same type of changes might be expected for the shear forces.

[78] However, as far as drying stresses are concerned, the stress reduction resulting from surfactant treatment should be about 50% since there is no detectable change in the dry modulus. This is true for blocks that previously get fully saturated. For blocks that are partially saturated, the tensile stresses can decrease by 40% at the most, but the stresses in this case are expected to be small unless the saturation is deep.

[79] Overall, these reductions in stresses, whether compressive, shear or tensile, are important in terms of avoiding or reducing the number of situations that can lead to damage. Such treatments should be considered as an option for monuments under the conditions discussed here. In addition, it is worth noting that if consolidation with ethyl silicates is to be considered, then a preliminary treatment with swelling reducing agents appears to be particularly advised. This should not be carried out without further testing; in particular, the effect that these products have on the stone strength at low loading rates should be investigated. However, applying swelling inhibitors to *Portland brownstone* before consolidation does indeed increase resistance to cycles of wetting and drying [*Scherer and Jiménez-González*, 2008].

[80] The reduction in swelling strain as well as in swelling stresses observed following the treatment with the swelling inhibitor, which adsorbs specifically on the clay minerals [*Snethlage and Wendler*, 1991], unambiguously demonstrates that the damage is associated with the expansion/shrinkage of these minerals. This is not a trivial conclusion, since controversy exists in the field of geomorphology as to the ultimate cause of wetting/drying damage in clay-containing sandstone, which has often been attributed to other weathering mechanisms, such as salt hydration/dehydration [*McGreevy and Smith*, 1984; *Turkington and Paradise*, 2005].

[81] Finally, it should be indicated that porosity and permeability of reservoir sandstones is drastically reduced because of swelling of clays, representing a significant problem in water injection or ''squeeze'' oil recovery [*Morris and Shepperd*, 1982; *Houseknecht and Pittman*, 1992; *Baker et al.*, 1993]. Different remediation treatments for this so-called formation damage, including the use of brines and surfactant polymer solutions, have been thoroughly studied and applied [*Borchardt*, 1989]. Our results suggest that the application of a diaminoalkane swelling inhibitor could be a potential solution for enhancing oil recovery in reservoir sandstones.

4.4. Implications for Understanding Sandstone Weathering in Nature

[82] The formation of several weathering forms observed in sandstone natural outcrops as well as in historic structures is poorly understood. This is the case of spalling and/or scaling/contour scaling, as well as polygonal cracking. Our results show that situations where damage can occur during wetting (and clay swelling) can lead to the formation of scales parallel to the exposed surface, as observed in Tarifa Church (Figure 9). Such a situation might explain why spalling and scaling/contour scaling are ubiquitous weathering forms in the sandstone monuments [*Snethlage and Wendler*, 1997] and in sandstone outcrops [*Campbell*, 1991; *Robinson and Williams*, 1994; *Turkington and Paradise*, 2005]. Previous theories suggesting that salt weathering is responsible for sandstone contour scaling [*Smith and McGreevy*, 1988], should therefore be reconsidered in lieu of these results. In addition, our results suggest that weathering phenomena associated with wetting events may contribute to tafoni development in salt-free sandstones, as has been suggested elsewhere [e.g., *Johnson*, 1974; *Martini*, 1978].

[83] On the other hand, drying stresses can lead to surface crack development (with cracks planes normal to the exposed surface), as observed in Tarifa Church (Figure 9b) and in nature [*Williams and Robinson*, 1989]. The latter striking weathering form, also-called ''polygonal cracks'' has also been observed in reworked evaporitic sandstones on Mars [*McLennan et al.*, 2005]. Figure 10 shows examples of such polygonal cracks developed on Martian rocks within Endurance Crater. The surface features are highly similar to those observed at Tarifa Church (Figure 9b). Those features point to stress development upon drying as a possible mechanism responsible for their formation.

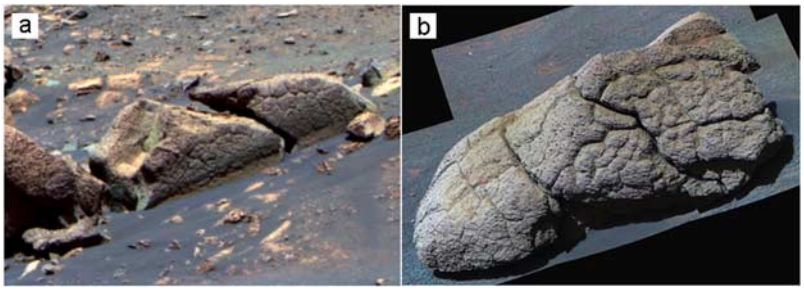

Figure 10. Polygonal cracks on sandstone rocks at Endurance crater, Meridiani Planum, Mars. (a) Pancam false color image of Earhart rock. Image is approximately 4 m across. This image was taken on Sol 219, sequence P1306, using 750, 530, and 430 nm filters. (b) False color Pancam mosaic of rock Wopmay within Endurance crater. Image is approximately 1 m across. Image was taken on Sol 251, sequence P2432, using 750, 530, and 430 nm filters. Image credits NASA/JPL/Cornell.

Potential minerals that could have been involved in the development of drying stresses could be magnesium sulfates [*Squyres et al.*, 2006] or clays, such as nontronite, chamosite, and montmorillonite, that several reports suggest are abundant on Martian surface rocks and sediments [*Poulet et al.*, 2005]. Interestingly, our theoretical analysis indicates that cracks would only develop when a significant portion of the rock is wet. This suggests that water could have been abundant on Mars' surface at the time of the formation of such weathering features.

[84] Note that controversy exists as to the origins of polygonal cracking in natural sandstone outcrops [*Williams and Robinson*, 1989]. It has been suggested that surface crusting due to deposition of secondary minerals and structural discontinuities between the crust and the substrate is the dominant process responsible for such a weathering form [*Turkington and Paradise*, 2005]. However, neither secondary minerals formation, nor crust development was observed in sandstone block displaying polygonal cracking in Tarifa Church [*Sebastián et al.*, 2008]. In contrast, crack formation upon drying appears to be sufficient to explain the formation of this striking weathering form.

[85] It should be stated that sandstones display a wide variation in mineralogy and texture, expanding from quartz arenites to arkoses, litharenites, and greywackes [*Tucker*, 1991]. In this respect, the *Tarifa sandstone* (an arkose) might not be fully representative of sandstones in general. However, nearly all sandstones include clays within the matrix, in proportions ranging from a few percent up to ~60 wt %, with an average value of ~10 wt % [*Tallman*, 1949]. The observed swelling/shrinking phenomena and the associated damage in Tarifa sandstone, with only 7 wt % clays, could thus be common for many of the sandstones on Earth's surface. In fact, extensive studies on swelling strains of a large number of sandstone types (~35) from many different locations show that nearly all sandstones experience some degree of hydric expansion, with values in the range 500–1000 μm/m on average, and maximum values of 5000–7000 μm/m for the clay-rich greywackes [*Felix*, 1983; *Esbert et al.*, 1997; *Snethlage and Wendler*, 1997; *Jiménez-González et al.*, 2002; *Heinrichs*, 2005].

[86] The extent of sandstone damage experienced upon wetting/drying cycles would depend, among other parameters, on exposure, textural anisotropy, clay content and type (i.e., presence of expandable clays as opposed to nonexpandable clays), and the interplay of other weathering phenomena. However, it is expected that the damage mechanism due to cyclic wetting and drying will in general terms follow the model presented here. In addition, this model may help explain many field observations regarding sandstone weathering: for instance, why weathering rates of sandstone landscapes typically show a positive correlation with the number of wetting/drying events [*Pentecost*, 1991], and why damage resulting in continuous scaling typically concentrates at the limit of rising damp [*Snethlage and Wendler*, 1997], where wetting/drying events are more frequent. The latter may explain the formation of large-scale sandstone weathering forms such as pedestal rocks, which have often been attributed to salt weathering [*Selby*, 1993].

5. Conclusions

[87] In this work, we have determined many material properties of *Tarifa sandstone* with the objective of supporting the analysis and validation of novel techniques used to characterize the swelling behavior of such a stone. These consist of the warping or "3 in 1" test on thin stone plates and an accelerated version of a swelling pressure measurement. Results show that the theory used to analyze these tests is valid, so that we may also apply it to calculate stresses than can develop in the field. Results of these calculations suggest that damage can take place in the two following ways:

[88] 1. Buckling and scaling/contour scaling development during wetting due to shear forces. This is enhanced by preexisting flaws that can be inherent to the stone (e.g., bedding planes) or result from other damage mechanisms, such as salt crystallization. It causes the detachment of rather large stone layers and is indeed something very evident on the façade that is the object of this study. Similar weathering forms are commonly observed in sandstone landscapes.

[89] 2. Tensile failure during drying. This type of damage only seems probable for thin ornamental elements that can get fully saturated or in sandstone outcrops where periods of wetting (rain showers, or capillary moisture uptake from the ground) are followed by intense drying. In those cases, the damage follows a mud-cracking pattern. This is also something that is observed on the ornaments of the San Mateo main Façade and on sandstone rocks, both on Earth and on Mars.

[90] Our stress analysis does not account for other types of damage reported by *Sebastián et al.* [2008], such as granular disintegration. In that case, those authors propose that the partially carbonatic nature of the cement in this sandstone could suffer chemical degradation caused by acid depositions from local traffic. The fact that wetting and drying would not account for that damage is supported by the fact that the same authors report it to occur in sheltered zones.

[91] Overall, our study clearly confirms that clay swelling and shrinkage is an important issue in the degradation of this monument and that swelling inhibitors have the potential of substantially reducing this type of damage. Similar weathering phenomena can also occur in natural sandstone outcrops, contributing to landscape modeling and evolution.

[92] Finally, it should be emphasized that the testing methodology and data analysis here presented and discussed might be a valuable tool for studying the response of different sandstone types to wetting/drying damage.

Appendix A: Drying Stress in Swelling Stone

[93] In this appendix we analyze the stresses generated during the drying of a partially wet stone block. We calculate what should be the depth of wetting in a stone block for these drying stresses to reach the tensile strength of the material. Consider a stone with thickness L that is wetted by water to a depth of $L_w + L_d$, after which the surface dries to a depth of L_d, as indicated in Figure A1. We calculate the stress in each zone. The x-y plane (which is the surface through which moisture passes) runs into the page, and the z axis is perpendicular to that surface. Since that surface is free, $\sigma_z = 0$; by symmetry, $\sigma_x = \sigma_y$ and $\varepsilon_x = \varepsilon_y$. If the free swelling strain is ε_s, then the constitutive equation of the stone is

$$\varepsilon_x = \varepsilon_f + \frac{1}{E_f}\left[\sigma_x - \nu_f\left(\sigma_y + \sigma_z\right)\right] = \varepsilon_f + \frac{\sigma_x\left(1-\nu_f\right)}{E_f}. \quad \text{(A1)}$$

[94] In the dry zone, $\varepsilon_f = 0$, $\nu_f = \nu_d$ and $E_f = E_d$; in the wet zone, $\varepsilon_f = \varepsilon_s$, $\nu_f = \nu_w$ and $E_f = E_w$. If the plate is wide compared to its thickness, L, then the strain ε_x will be the same in each region. We assume that the plate is prevented from warping (which is strictly true only if the wet region is exactly in the middle, so that the stresses are symmetrical), and that the edges are free. If there is no net force on the edges, then

$$\int_0^L \sigma_x dz = 0 \quad \text{(A2)}$$

the stress is

$$\sigma_x = \left(\frac{E_f}{1-\nu_f}\right)\left(\varepsilon_x - \varepsilon_f\right) = \begin{cases} \left(\frac{E_d}{1-\nu_d}\right)\varepsilon_x, 0 \le z \le L_d \\ \left(\frac{E_w}{1-\nu_w}\right)\left(\varepsilon_x - \varepsilon_s\right), L_d < z \le L_d + L_w, \\ \left(\frac{E_d}{1-\nu_d}\right)\varepsilon_x, L_d + L_w \le z \le L \end{cases} \quad \text{(A3)}$$

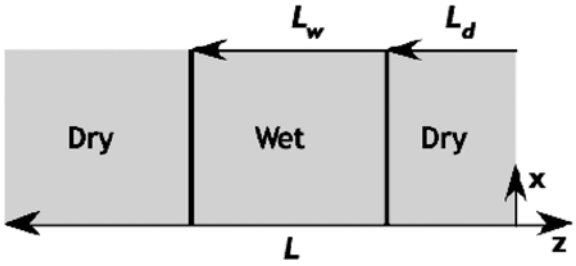

Figure A1. Illustration of the wet and dry parts of the stone block considered to analyze drying stresses in a partially wet block.

so if the Poisson ratio is assumed to be the same in both regions, equation (12) leads to

$$\varepsilon_x = \varepsilon_s\left(\frac{r}{r + \left(\frac{L - L_w}{L_w}\right)}\right), \quad \text{(A4)}$$

where $r = E_w/E_d$. The stress in the drying region is

$$\sigma_{d,2} = \frac{E_d\varepsilon_S}{1-\nu_d}\left(\frac{r}{r + \frac{L - L_w}{L_w}}\right), \quad \text{(A5)}$$

which is equation (10) in section 4.3.2.

[95] When $L_w = 0$, there is no swelling, so $\sigma_{d,2} = 0$; as L_w approaches L, the dry region is very thin so the contraction is completely suppressed and the stress in the dry region achieves its maximum value

$$\sigma_d = \left(\frac{E_d\varepsilon_s}{1-\nu_d}\right), \quad \text{(A6)}$$

which is equation (9) in section 4.3.2.

Notation

a, b	fitting constants for the dry viscoelastic modulus (GPa).
A	sample base in a sorptivity experiment (cm^2)
d	relative depth of water penetration in a warping sample (dimensionless)
E_f	elastic modulus, E_d in the dry zone and E_w in the wet zone (see Appendix A) (GPa)
$E_d(t)$, $E_w(t)$	viscoelastic modulus respectively of the dry and wet stone at time t (GPa)
E_d, E_w	elastic modulus respectively of the dry and wet stone, corresponding also to $E_d(t)$ and $E_w(t)$ at $t = 0$ (GPa)
h	plate thickness in a warping experiment (cm)
h_w	wet part of the sample thickness in a warping experiment (cm)
L	stone thickness of a partially saturated stone (cm)
L_d, L_w	depth of dry and wet part of a partially saturated stone of thickness L (cm)
r	ratio of wet to dry modulus (E_w/E_d) (dimensionless)

r_i, r_o inner and outer radius respectively of a swelling pressure measurement sample (cm)
$R(t)$ hydrodynamic relaxation function of a wet stone in a bending experiment (dimensionless)
S sorptivity (cm/s$^{1/2}$)
t time (s)
t_{sat} saturation time in swelling pressure test (s)
w span in a warping test (cm)
$W(t)$, $W(0)$ load in a beam bending experiment at time t and $t = 0$ respectively (g)
β fitting parameter of the viscoelastic relaxation function (dimensionless)
Δ warping deflection (cm or μm)
Δ_{max} maximum warping deflection (cm or μm)
Δh average height of water rise in a sorptivity experiment (cm)
Δm mass change in a sorptivity experiment (g)
ε_f swelling strain in a zone of a partially saturated stone; equals to zero in the dry zone and to ε_S in the wet zone (dimensionless)
ε_S free swelling strain (dimensionless or μm/m)
ε_x strain in an (x-y) plane parallel to the drying surface (dimensionless)
ϕ porosity
ν_d, ν_w Poisson's ratio of the dry and wet stone respectively (dimensionless)
ν_f Poisson's ratio in a zone of a partially saturated stone; equals to ν_d, in the dry zone and to ν_w in the wet one (dimensionless)
ρ_L liquid density (g/cm^3)
σ_d maximum tensile stresses expected during drying (MPa)
σ_w maximum compressive stresses during wetting (MPa)
$\sigma_{d,2}$ tensile stress in the drying part of a partially saturated stone (MPa)
σ_x, σ_y, σ_z stresses in the plane parallel to the drying surface (x-y) and in the direction perpendicular to it (z) (MPa)
τ_1, τ_2 characteristic times of the first and second relaxation regimes of the dry stone (s)
τ_{VE} characteristic time for viscoelastic relaxation of the wet stone (s)
$\psi(t)$ viscoelastic relaxation function of the wet stone (dimensionless)

[96] **Acknowledgments.** Financial support for Inmaculada Jiménez-González was provided by the Samuel Kress Foundation and VIP Restoration, Inc. The authors would also like to thank Dr. Giuseppe Cultrone, the corresponding author of the paper by *Sebastián et al.* [2008], for sharing very useful information from that paper before its publication. One of us (C.R.-N.) acknowledges the financial support provided by the Spanish Government under contract MAT2006-00578 and by the Research Group RNM-179 (Junta de Andalucia, Spain).

References

Baker, J. C., P. J. R. Uwins, and I. D. R. Mackinnon (1993), ESEM study of illite/smectite freshwater sensitivity in sandstone reservoirs, *J. Petrol. Sci. Eng.*, *9*, 83–94, doi:10.1016/0920-4105(93)90069-Q.

Beloyiannis, N., P. Theoulakis, and L. Haralambides (1988), Causes and mechanism of stone alteration at the temple of Apollo Epicuros, in *Engineering Geology of Ancient Works, Monuments and Historic Sites*, edited by P. Marinos and G. Koukis, pp. 763–770, Balkema, Rotterdam, Netherlands.

Borchardt, J. K. (1989), Chemicals used in oil-field operations, *ACS Symp. Ser.*, *396*, 3–54.

Bradley, W. C. (1963), Large-scale exfoliation in massive sandstones of the Colorado plateau, *Geol. Soc. Am. Bull.*, *74*, 519–528, doi:10.1130/0016-7606(1963)74[519:LEIMSO]2.0.CO;2.

Campbell, I. A. (1991), Classification of rock weathering at Writing-on-Stone Provincial Park, Alberta, Canada: A study in applied geomorphology, *Earth Surf. Processes Landforms*, *16*, 701–711, doi:10.1002/esp.3290160804.

Caner, E. N., and N. J. Seeley (1978), The clay minerals and the decay of limestone, paper presented at International Symposium on Deterioration and Protection of Stone Monuments, UNESCO-RILEM, Paris.

Cruikshank, K. M., and A. Aydin (1994), Role of fracture localization in arch formation, Arches National Park, *Utah, Geol. Soc. Am. Bull.*, *106*, 879–891, doi:10.1130/0016-7606(1994)106<0879:ROFLIA>2.3.CO;2.

Delgado Rodrigues, J. (2001), Swelling behaviour of stones and its interests in conservation: An appraisal, *Mater. Constr.*, *51*, 263–264.

Dragovich, D. (1978), Building stone and its use in rock weathering studies, *J. Geol. Educ.*, *27*, 21–25.

Dunn, J. R., and P. P. Hudec (1966), Water, clay and rock soundness, *Ohio J. Sci.*, *66*, 153–168.

Dunning, J. D., and W. L. Huf (1983), The effects of aqueous chemical environments on crack and hydraulic fracture propagation and morphologies, *J. Geophys. Res.*, *88*(B8), 6491–6499, doi:10.1029/JB088iB08p06491.

Dunning, J. D., W. L. Lewis, and W. L. Huf (1980), Chemomechanical weakening in the presence of surfactants, *J. Geophys. Res.*, *85*(B10), 5344–5354, doi:10.1029/JB085iB10p05344.

Esbert, R. M., J. Ordaz, F. J. Alonso, M. Montoto, T. González Limón, and M. Alvarez de Buergo Ballester (1997), *Manual de Diagnosis y Tratamiento de Materials Pétreos y Cerámicos*, 130 pp., Coll. Aparelladors Arquitectes Tèc. Barcelona, Barcelona, Spain.

Felix, C. (1983), Sandstone linear swelling due to isothermal water sorption, in *Materials Science and Restoration*, edited by F. H. Wittmann, pp. 305–310, Tech. Akad. Esslingen, Ostfildern, Germany.

Félix, C. (1988), Comportement des grès en construction sur le plateau Suisse, in *Conservation et Restauration des Biens Culturels*, edited by R. Pancella, pp. 833–841, Ecole Polytech. Fed. Lausanne, Montreux, Switzerland.

Félix, C. (1995), Choix de gres tenders du Plateau Suisse pour les travaux de conservation, in *Conservation et Restauration des Biens Culturels*, edited by R. Pancella, pp. 45–71, Ecole Polytech. Fed. Lausanne, Montreux, Switzerland.

Félix, C., and V. Furlan (1994), Variations dimensionnelles des gres et calcaires liees a leur consolidation avec un silicate d'ethyle, in *Proceedings of the 3rd International Symposium on the Conservation of Monuments in the Mediterranean Basin*, edited by V. Fassina and F. Zezza, pp. 855–859, Graffo, Venice, Italy.

Fookes, P. G., and A. B. Poole (1981), Some preliminary considerations on the selection and durability of rock and concrete materials for breakwaters and coastal protection work, *Q. J. Eng. Geol. Hydrogeol.*, *14*, 97–128, doi:10.1144/GSL.QJEG.1981.014.02.03.

Gill, E. D., E. R. Segnit, and N. H. McNeill (1980), Rate of honeycomb weathering features (small scale tafoni) on the Otway Coast, S.E. Australia, *Proc. R. Soc. Victoria*, *92*, 149–154.

Goudie, A. S., and H. Viles (1997), *Salt Weathering Hazards*, 241 pp., John Wiley, Oxford, UK.

Hall, K., and A. Hall (1996), Weathering by wetting and drying: some experimental results, *Earth Surf. Processes Landforms*, *21*, 365–376, doi:10.1002/(SICI)1096-9837(199604)21:4<365::AID-ESP571>3.0.CO;2-L.

Heinrichs, K. (2005), Diagnose der Verwitterungsschäden an den Felsmonumenten der antiken Stadt Petra, Jordanien, Ph.D. dissertation, Aachener Geowiss. Beitr., Aachen, Germany.

Hoke, G. D., and D. L. Turcotte (2002), Weathering and damage, *J. Geophys. Res.*, *107*(B10), 2210, doi:10.1029/2001JB001573.

Houseknecht, D. W., and E. D. Pittman (Eds.) (1992), *Origin, Diagenesis, and Petrophysics of Clay Minerals in Sandstones*, *SEMP Spec. Publ.*, vol. 47, SEMP, Tulsa, Okla.

Hoyos, M., S. Sanchez-Moral, E. Sanz-Rubio, and J. C. Cañaveras (1999), Alteration causes and processes in the stone material from the pavement in Baelo Claudia archaeological site, Cádiz/Spain, *Mater. Constr.*, *49*, 5–18.

Iñigo, A. C., J. García-Talegón, R. Trujillano, E. Molina, and V. Rives (2003), Evolution and decay processes in the Villamayor and Zamora sandstones, in *Applied Study of Cultural Heritage and Clays*, edited by J. L. Perez-Rodríguez, pp. 47–57, Cons. Super. Invest. Cient., Sevilla, Spain.

Jiménez-González, I., and G. W. Scherer (2004), Effect of swelling inhibitors on the swelling and stress relaxation of clay bearing stones, *Environ. Geol.*, *46*, 364–377, doi:10.1007/s00254-004-1038-8.

Jiménez-González, I., and G. W. Scherer (2006), Evaluating the potential damage to stones from wetting and drying cycles, in *Measuring, Monitoring and Modeling Concrete Properties*, edited by M. S. Konsta-Gdoutos, pp. 685–693, Springer, Dordrecht, Netherlands.

Jiménez-González, I., M. Higgins, and G. W. Scherer (2002), Hygric swelling of Portland Brownstone, *Mater. Res. Soc. Symp. Proc.*, *712*, 21–27.

Johnson, A. R. M. (1974), Cavernous weathering at Berowra, N.S.W., *Aust. Geogr.*, *12*, 531–535, doi:10.1080/00049187408702665.

Kühnel, R. A., S. J. Van der Gaast, J. Brych, G. J. Laan, and H. Kulnig (1994), The role of clay minerals in durability of rocks observation on basaltic rocks, *Appl. Clay Sci.*, *9*, 225–237, doi:10.1016/0169-1317(94)90001-9.

Madsen, F. T., and M. Müller-Vonmoos (1985), Swelling pressure calculated from mineralogical properties of a jurassic opalinum shale, Switzerland, *Clays Clay Miner.*, *33*, 501–509, doi:10.1346/CCMN.1985.0330604.

Madsen, F. T., and M. Müller-Vonmoos (1989), The swelling behaviour of clays, *Appl. Clay Sci.*, *4*, 143–156, doi:10.1016/0169-1317(89)90005-7.

Martini, I. P. (1978), Tafoni weathering, with examples of Tuscany, Italy, *Z. Geomorphol.*, *22*, 44–67.

McGreevy, J. P. (1981), Some perspectives on frost shattering, *Prog. Phys. Geogr.*, *5*, 56–75, doi:10.1177/030913338100500103.

McGreevy, J. P., and B. J. Smith (1984), The possible role of clay minerals in salt weathering, *Catena*, *11*, 169–175.

McGreevy, J. P., and W. B. Whalley (1984), Weathering, *Prog. Phys. Geogr.*, *8*, 543–569, doi:10.1177/030913338400800404.

McLennan, S. M., et al. (2005), Provenance and diagenesis of the evaporite-bearing Burns formation, Meridiani Planum, Mars, *Earth Planet. Sci. Lett.*, *240*, 95–121, doi:10.1016/j.epsl.2005.09.041.

Meierding, T. C. (1981), Marble tombstone weathering rates: A transect of the United States, *Phys. Geogr.*, *2*, 1–18.

Meybeck, M. (1987), Global chemical weathering of surficial rocks estimated from river dissolved loads, *Am. J. Sci.*, *287*, 401–428.

Morris, K. A., and C. M. Shepperd (1982), The role of clay minerals in influencing porosity and permeability characteristics in the Bridport Sands of Wytch Farm, Dorset, *Clay Miner.*, *17*, 41–54, doi:10.1180/claymin.1982.017.1.05.

Mottershead, D., A. Gorbushina, G. Lucas, and J. Wright (2003), The influence of marine salts, aspect and microbes in the weathering of sandstone in two historic structures, *Building Environ.*, *38*, 1193–1204, doi:10.1016/S0360-1323(03)00071-4.

Mustoe, G. E. (1982), The origin of honeycomb weathering, *Geol. Soc. Am. Bull.*, *93*, 108–115, doi:10.1130/0016-7606(1982)93<108:TOOHW>2.0.CO;2.

Paradise, T. R. (2002), Sandstone weathering and aspect in Petra, Jordan, *Z. Geomorphol.*, *46*, 1–17.

Pentecost, A. (1991), The weathering rates of some sandstone cliffs, central Weald, England, *Earth Surf. Processes Landforms*, *16*, 83–91, doi:10.1002/esp.3290160109.

Pope, G. A., T. C. Meierding, and T. R. Paradise (2002), Geomorphology's role in the study of the weathering of cultural stone, *Geomorphology*, *47*, 211–225, doi:10.1016/S0169-555X(02)00098-3.

Poulet, F., et al. (2005), Phyllosilicates on Mars and implications for early Martian climate, *Nature*, *438*, 623–627, doi:10.1038/nature04274.

Pye, K., and D. N. Mottershead (1995), Honeycomb weathering of Carboniferous sandstone in a sea wall at Weston-super-Mare, UK, *Q. J. Eng. Geol.*, *28*, 333–347, doi:10.1144/GSL.QJEGH.1995.028.P4.03.

Robinson, D. A., and D. A. Williams (1994), Sandstone weathering and landforms in Britain and Europe, in *Weathering and Landform Evolution*, edited by D. A. Robinson and R. B. G. Williams, pp. 371–391, John Wiley, Chichester, UK.

Robinson, E. S. (1970), Mechanical disintegration of the Navajo sandstone in Zion Canyon, Utah, *Geol. Soc. Am. Bull.*, *81*, 2799–2806, doi:10.1130/0016-7606(1970)81[2799:MDOTNS]2.0.CO;2.

Rodríguez-Navarro, C., and E. Doehne (1999), Salt weathering: Influence of evaporation rate, supersaturation and crystallization pattern, *Earth Surf. Processes Landforms*, *24*, 191–209, doi:10.1002/(SICI)1096-9837(199903)24:3<191::AID-ESP942>3.0.CO;2-G.

Rodríguez-Navarro, C., E. Hansen, E. Sebastián Pardo, and W. S. Ginell (1997), The role of clays in the decay of ancient Egyptian limestone sculptures, *J. Am. Inst. Conserv.*, *36*, 151–163, doi:10.2307/3179829.

Rodríguez Navarro, C., E. Sebastián, E. Dohene, and W. S. Ginell (1998), The role of sepiolite-palygorskite in the decay of ancient Egyptian limestone sculptures, *Clays Clay Miner.*, *46*, 414–422, doi:10.1346/CCMN.1998.0460405.

Sancho, C., and G. Benito (1990), Factors controlling tafoni weathering in the Ebro Basin (NE Spain), *Z. Geomorphol.*, *34*, 165–177.

Scherer, G. W. (2000), Stress from crystallization of salt in pores, in *Proceedings of the* 9th *International Congress on Deterioration and Conservation of Stone*, edited by V. Fassina, pp. 187–194, Elsevier Sci., Amsterdam.

Scherer, G. W. (2004), Measuring permeability of rigid materials by a beam-bending method: part IV. Transversely isotropic plate, *J. Am. Ceram. Soc.*, *87*, 1517–1524.

Scherer, G. W. (2006), Internal stress and cracking in stone and masonry, in *Measuring, Monitoring and Modeling Concrete Properties*, edited by M. S. Konsta-Gdoutos, pp. 633–641, Springer, Dordrecht, Netherlands.

Scherer, G. W., and I. Jiménez-González (2005), Characterization of swelling in clay-bearing stone, in *Stone Decay in the Architectural Environment*, *Geol. Soc. Am. Spec. Pap.*, vol. 390, edited by A. V. Turkington, pp. 51–61, Geol. Soc. of Am., Boulder, Colo.

Scherer, G. W., and I. Jiménez-González (2008), Swelling clays and salt crystallization: The damage mechanisms and the role of consolidants, paper presented at International Symposium on Stone Consolidation in Cultural Heritage, Lab. Nac. de Engenharia Civ., Lisbon.

Sebastián, E., G. Cultrone, D. Benavente, C. Rodríguez Navarro, and L. Linares (2008), Swelling damage in clay-rich sandstones used in Architectural Heritage, *J. Cult. Herit.*, *9*, 66–76.

Selby, M. J. (1993), *Hillslope Materials and Processes*, 2nd ed., 451 pp., Oxford Univ. Press, Oxford, UK.

Smith, B. J., and J. P. McGreevy (1988), Contour scaling of sandstone by salt weathering under simulated hot desert conditions, *Earth Surf. Processes Landforms*, *13*, 697–705, doi:10.1002/esp.3290130804.

Smith, B. J., R. W. Magee, and W. B. Whalley (1994), Breakdown patterns of quartz sandstone in a polluted urban environment, Belfast, Northern Ireland, in *Rock Weathering and Landform Evolution*, edited by D. A. Robinson and R. B. G. Williams, pp. 131–150, John Wiley, Chichester, UK.

Snethlage, R., and E. Wendler (1991), Surfactants and adherent silicon resins—New protective agents for natural stone, *Mater. Res. Soc. Symp. Proc.*, *185*, 193–200.

Snethlage, R., and E. Wendler (1997), Moisture cycles and sandstone degradation, in *Saving Our Architectural Heritage: The Conservation of Historic Stone Structures*, edited by N. S. Baer and R. Snethlage, pp. 7–24, John Wiley, London.

Squyres, S. W., et al. (2006), Two years at Meridiani Planum: Results from the Opportunity Rover, *Science*, *313*, 1403–1407, doi:10.1126/science.1130890.

Tallman, S. L. (1949), Sandstone types: Their abundance and cementing agents, *J. Geol.*, *57*, 582–591.

Timoshenko, S. (1925), Analysis of bimetal thermostats, *J. Opt. Soc. Am.*, *11*, 233–255.

Trenhaile, A. S. (1987), *The Geomorphology of Rock Coasts*, 384 pp., Clarendon, Oxford, UK.

Tucker, M. E. (1991), *Sedimentary Petrology: An Introduction to the Origin of Sedimentary Rocks*, 2nd ed., 260 pp., Blackwell Sci., Oxford, U. K.

Turkington, A. V., and T. R. Paradise (2005), Sandstone weathering: A century of research and innovation, *Geomorphology*, *67*, 229–253, doi:10.1016/j.geomorph.2004.09.028.

Veniale, F., M. Setti, C. Rodríguez-Navarro, and S. Lodola (2001), Role of clay constituents in stone decay processes, *Mater. Constr.*, *51*, 163–182.

Vicente, M. A. (1983), Clay mineralogy as the key factor in weathering of 'Arenisca dorada' (Golden sandstone) of Salamanca, Spain, *Clay Miner.*, *18*, 215–217, doi:10.1180/claymin.1983.018.2.11.

Vichit-Vadakan, W. (2002), Measuring permeability, young modulus and stress relaxation by the beam-bending technique, Ph.D. Dissertation, Princeton Univ. Princeton, N. J.

Vichit-Vadakan, W., and G. W. Scherer (2000), Measuring permeability of rigid materials by a beam-bending method: part II. Porous glass, *J. Am. Ceram. Soc.*, *83*, 2240–2245.

Vichit-Vadakan, W., and G. W. Scherer (2002), Measuring permeability of rigid materials by a beam-bending method: part III. Cement paste, *J. Am. Ceram. Soc.*, *85*, 1537–1544.

von Engeln, O. D. (1942), *Geomorphology: Systematic and Regional*, 655 pp., Macmillan, New York.

Wangler, T. P., A. K. Wylykanowitz, and G. W. Scherer (2006), Controlling stress from swelling clay, in *Measuring, Monitoring and Modeling Concrete Properties*, edited by M. S. Konsta-Gdoutos, pp. 703–708, Springer, Dordrecht, Netherlands.

Warke, P. A., and B. J. Smith (1998), Effects of direct and indirect heating on the validity of rock weathering simulation studies and durability tests, *Geomorphology*, *22*, 347–357, doi:10.1016/S0169-555X(97)00078-0.

Wendler, E., D. D. Klemm, and R. Snethlage (1991), Consolidation and hydrohobic treatment of natural stone, in *Durability of Building Materials and Components: Proceedings of the 5th International Conference*, edited by J. M. Baker et al., pp. 203–212, Chapman and Hall, London.

Wendler, E., A. E. Charola, and B. Fitzner (1996), Easter Island tuff: Laboratory studies for its consolidation, in *Proceedings of the 8th International Congress on Deterioration and Conservation of Stone*, edited by J. Riederer, pp. 1159–1170, Elsevier Sci., Berlin.

Williams, R., and D. Robinson (1989), Origin and distribution of polygonal cracking of rock surfaces, *Geogr. Ann. Ser. A*, *71*, 145–151, doi:10.2307/521386.

Wilson, M. J. (1987), *A Handbook of Determinative Methods in Clay Mineralogy*, 308 pp., Chapman and Hall, New York.

Winkler, E. M. (1997), *Stone in Architecture: Properties, Durability*, 3rd ed., 313 pp., Springer-Verlag, Berlin.

Wüst, R. A. J., and J. McLane (2000), Rock deterioration in the royal tomb of Seti I, Valley of the Kings, Luxor, Egypt, *Eng. Geol.*, *58*, 163–190, doi:10.1016/S0013-7952(00)00057-0.

Yatsu, E. (1988), *The Nature of Weathering: An Introduction*, 624 pp., Sozosha, Tokyo.

Young, A. R. (1987), Salt as an agent in the development of cavernous weathering, *Geology*, *15*, 962–966, doi:10.1130/0091-7613(1987)15<962:SAAAIT>2.0.CO;2.

I. Jiménez-González, University of Granada, Fuentenueva s/n, 18002 Granada, Spain. (inmajimenez@ugr.es)

C. Rodríguez-Navarro, Department of Mineralogy and Petrology, University of Granada, Fuentenueva s/n, 18002 Granada, Spain. (carlosrn@ugr.es)

G. W. Scherer, Princeton Institute for the Science and Technology of Materials, Department of Civil and Environmental Engineering, Princeton University, 321 Bowen Hall, 70 Prospect Avenue, Princeton, NJ 08540, USA. (scherer@princeton.edu)